Journal of Magnetism and Magnetic Materials 490 (2019) 165443

Contents lists available at ScienceDirect

Journal of Magnetism and Magnetic Materials

journal homepage: www.elsevier.com/locate/jmmm

Research articles

Enhancement of magnetoresistance and magnetocaloric effect at room temperature in polycrystalline $Pr_{0.8-x}La_xSr_{0.2}MnO_3$ ($x = 0.2$) compound

Sanjib Banik[a,*,1], Kalipada Das[b], I. Das[a]

[a] CMP Division, Saha Institute of Nuclear Physics, HBNI, 1/AF-Bidhannagar, Kolkata 700 064, India
[b] Department of Physics, Seth Anandram Jaipuria College, 10, Raja Naba Krishna Street, Kolkata 700005, India

A B S T R A C T

The effect of chemical pressure on the ferromagnetic insulator ground state and its effect on magnetotransport and magnetocaloric properties has been explored in this study. Magnetic and magnetotransport measurements reveal that the increased chemical pressure in $Pr_{0.6}La_{0.2}Sr_{0.2}MnO_3$ due to the partial substitution by La in $Pr_{0.8}Sr_{0.2}MnO_3$ compound change the low-temperature insulator phase to the metallic phase. A room temperature enhancement of magnetoresistance (MR), as well as large relative cooling power (RCP), have been achieved with increasing chemical pressure in $x = 0.2$ compound. This enhancement of MR and magnetocaloric effect (MCE) in $Pr_{0.6}La_{0.2}Sr_{0.2}MnO_3$ compound have been attributed to the short- range ferromagnetic cluster formation at higher temperature ($T > T_C$).

1. Introduction

During the last two decades, doped perovskite manganites $RE_{1-x}A_xMnO_3$ have attracted considerable attention due to their fascinating physical properties, arising from its strong interplay between different degrees of freedom [1–10]. Besides the interesting physical properties, these systems also exhibit intriguing functional properties, viz., colossal magnetoresistance (CMR) [2,3,11,12] and magnetocaloric effect (MCE) [13–15], which have applications in magnetic field sensor and in magnetic refrigeration technology (MRT) respectively. Magnetoresistance is the change in resistance on the application of the external magnetic field and MCE is generally quantified by the isothermal change of magnetic entropy (ΔS_M) or the adiabatic temperature change (ΔT_{ad}) of a system due to the influence of external magnetic field. For application perspectives, besides ΔS_M and ΔT_{ad}, another important parameter for the MCE material is the relative cooling power (RCP) [16–18]. It is the amount of heat transfer from the hot end to the cold end in an ideal refrigeration cycle. Nowadays, MCE have gained an acute attention of the researcher due to its potential application in environment-friendly and energy saving magnetic refrigeration technique and being a promising alternative of the conventional gas compression refrigeration technology. For technological perspectives, searching for materials having large MCE with a wider range of operating temperature and magnetoresistance at room temperature have become the most important topics during previous few years [19–24].

Generally, large magnetoresistance and large magnetocaloric effect are observed at the vicinity of the magnetic phase transitions [25–29]. Therefore to observe large magnetoresistance and MCE near room temperature, the ordering temperature of the sample has to be near to the room temperature. Again from MCE point of view high resistive materials are suitable due to minimization of eddy current losses [30]. One of such high resistive material is the ferromagnetic insulator (FMI). The phase diagram in the Fig. 1 (generated from the reported literatures [4,9,31,32]) for the different FMI manganites at the hole doping $x = 0.2$ shows a clear crossover from ferromagnetic insulator (FMI) to ferromagnetic metallic (FMM) phase with increasing A-site ionic radius $\langle r_A \rangle$. So here our idea is to prepare a sample near to this phase boundary to see the effect of chemical pressure and the corresponding changes in the physical properties.

For this particular doping concentration ($x = 0.2$) with reduction of the temperature, $Pr_{0.8}Sr_{0.2}MnO_3$ undergoes paramagnetic to ferromagnetic insulator transition (FMI) whereas $La_{0.8}Sr_{0.2}MnO_3$ shows the ferromagnetic metallic transition (FM). However, for $La_{0.8}Sr_{0.2}MnO_3$, the ordering temperature (Curie temperature, T_C) is greater compared to $Pr_{0.8}Sr_{0.2}MnO_3$[9,33]. From the aspect of the magnetocaloric effect, though the ordering temperature of $La_{0.8}Sr_{0.2}MnO_3$ compound is near to the room temperature but due to the higher effective magnetic moment, $Pr_{0.8}Sr_{0.2}MnO_3$ compound is more important. Considering the above mentioned facts it may be an interesting study to see the effect of chemical pressure to destabilize the ferromagnetic insulator ground state when Pr-site in $Pr_{0.8}Sr_{0.2}MnO_3$ compound is slightly substitutes by 'La' ions. Recently Zhang *et al.* reported the interesting route where La-site was gradually substituted by 'Pr' in $La_{0.7-x}Pr_xMnO_3$ compound and ordering temperature (T_C) shifted towards low temperature[34].

* Corresponding author.
E-mail address: sanjib.banik@physik.uni-wuerzburg.de (S. Banik).
[1] Present address: University of Würzburg, Am Hubland, 97074 Würzburg, Germany.

https://doi.org/10.1016/j.jmmm.2019.165443
Received 7 March 2019; Received in revised form 5 May 2019; Accepted 10 June 2019
Available online 29 June 2019

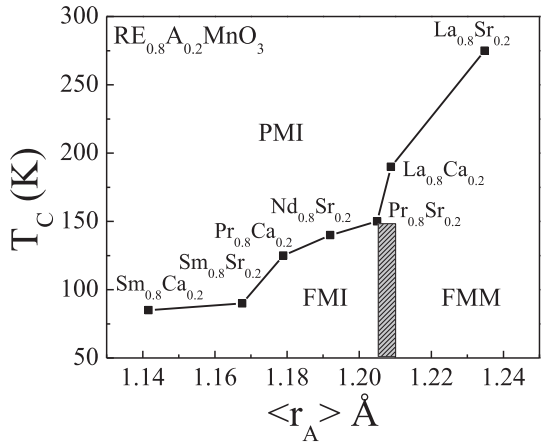

Fig. 1. Phase diagram of manganites $RE_{0.8}A_{0.2}MnO_3$. Here PMI: Paramagnetic insulator, FMM: Ferromagnetic metal and FMI: Ferromagnetic insulator, Hatched region: FMO-FMM overlapping region.

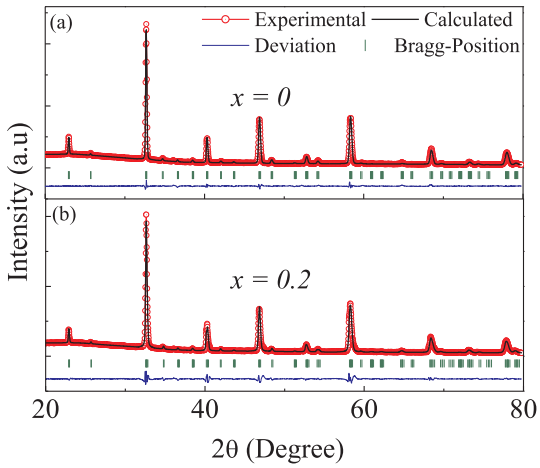

Fig. 2. Room temperature X-ray diffraction data with its profile fitted data for the polycrystalline compounds $Pr_{0.8-x}La_xSr_{0.2}MnO_3$ (a) $x = 0$ and (b) $x = 0.2$.

However, in our present study we have chosen Pr-rich $Pr_{0.8}Sr_{0.2}MnO_3$ compound and a slightly further A-site doped $Pr_{0.6}La_{0.2}Sr_{0.2}MnO_3$ polycrystalline compound. The parent compound $Pr_{0.8}Sr_{0.2}MnO_3$ was considered due to the ferromagnetic ground state below 100 K. However by La-doping in Pr-site due to the lattice distortion it is expected the behavior should be opposite as reported by Zhang et al.[34].

Our experimental outcome shows that though the numerical value of the ΔS_M is larger for $Pr_{0.8}Sr_{0.2}MnO_3$ compound but the span of the temperature in magnetocaloric entropy distribution is wider in the prepared $Pr_{0.6}La_{0.2}Sr_{0.2}MnO_3$ polycrystalline compound. We have also seen an enhancement of magnetoresistance in the La-doped compound. Our experimental results were analyzed considering the existence of short range ferromagnetic clusters in the broadened temperature range in case of $Pr_{0.6}La_{0.2}Sr_{0.2}MnO_3$ polycrystalline compound. This study shows a pathway to enhance the MR as well as ΔS_M at the room temperature and also the efficiency of the MCE material.

2. Sample preparation and characterization

All the polycrystalline bulk $Pr_{0.8-x}La_xSr_{0.2}MnO_3$ ($x = 0$, 0.2) compounds were prepared by the standard sol–gel method with an appropriate amount of Pr_6O_{11} (or Pr_6O_{11} and La_2O_3), $Sr(NO_3)_2$ and MnO_2 as the starting materials of purity greater than 99.9%. To prepare the bulk samples, the decomposed gel was pelletized and subsequently sintered at 1300^0C in the air for 36 h.

To characterize the samples, room temperature X-ray diffraction study was carried out using a Rigaku TTRAX-III diffractometer with Cu-K_α radiation of wave length $\lambda = 1.54$ Å. To perform the magnetic and magnetocaloric properties, a superconducting quantum interference device (SQUID) magnetometer (Quantum Design) was used. Electronic transport and magneto-transport measurements were carried out by four probe method in longitudinal geometry by utilizing a cryogenics magnet system and a homemade insert.

3. Experimental results and discussion

Room temperature X-ray diffraction study presented in Fig. 2 indicates the single phase nature of the compounds. From profile fitting (using *Pbnm* space group symmetry) using FULLPROF software of the X-ray diffraction data, we have extracted the lattice parameters and unit cell volume for the compounds (see Table 1). An increase in unit cell volume has been observed in the La-doped compound which is due to the partial substitution of Pr with higher ionic radii La. From the extracted lattice parameters, we have also calculated the orthorhombic distortions ($\Delta = \frac{a+b-c/\sqrt{2}}{a+b+c/\sqrt{2}}$) and it comes out to be 0.3342 and 0.3323 for $x = 0$ and $x = 0.2$ compounds respectively.

Table 1
The lattice parameters and unit cell volume of the samples $Pr_{0.8-x}La_xSr_{0.2}MnO_3$ ($x = 0$, 0.2).

x	a (Å)	b (Å)	c (Å)	V (Å^3)
0	5.4893	5.4795	7.7413	232.851
0.2	5.4937	5.4634	7.7656	233.085

Manganites being a strongly correlated system, the reduction of lattice distortion will also be reflected in the transport as well as in magnetotransport properties. Thus we have performed temperature dependent resistivity for both the samples in zero field as well as in 70 kOe external magnetic field (see Fig. 3). With decreasing the temperature $Pr_{0.8}Sr_{0.2}MnO_3$ compound shows insulating nature in the presence and in the absence of external magnetic field. However, due to the La-doping in Pr-site, the ground state of the material transform into a metallic state at the low-temperature region. The magnetic field in both the samples have very minute effect. Although at low temperature ($T < 250$ K) resistivity decreases in the La doped compound but there is an increase in the residual resistivity in the La-doped compound at higher temperature ($T > 250$ K).

To see the effect of external magnetic field in the high-temperature region, we have performed the isothermal resistivity measurement with magnetic field at 300 K. From these data, magnetoresistance (MR) of both samples have been calculated using the relation $MR(\%) = [R(H)/R(0) - 1] \times 100$ and is plotted in Fig. 3(b). An increase in the MR has been observed from 15% to the 26% due to the partial substitution of La in place of Pr. Another point here needs to mention that, the curvature of MR vs. H curves also changes from convex to concave. This concave nature indicates the presence of some kind of ferromagnetic interaction at 300 K in the La doped sample. To further investigate the basic physics behind this enhancement of MR in the La doped compound, we have analyzed the MR data with the help of spin-polarized tunneling model (SPT)[35]. According to this model, the expression of MR is

$$MR = -A' \int_0^H f(k)dk - JH - KH^3 \quad (1)$$

In the absence of magnetic field ferromagnetic domains are pinned at the grain boundary with pinning strength k having following distribution

$$f(k) = Aexp(-Bk^2) + Cexp(-Dk^2) \quad (2)$$

After determining all these adjustable fitting parameters, MR_{SPT} and

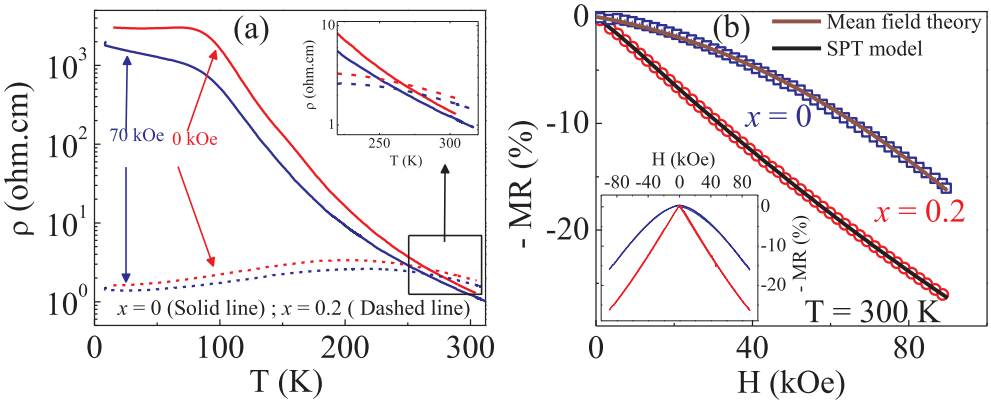

Fig. 3. (a) Temperature dependent resistivity of $Pr_{0.8-x}La_xSr_{0.2}MnO_3$ (x = 0.0, 0.2) compounds in presence of 0 kOe and 70 kOe external magnetic fields. Inset is the enlarge view of the same near the room temperature. (b) Plot of MR vs. H at 300 K for both the samples and its fitting with different model where black and brown solid lines are the fitted lines. Inset shows the corresponding five quadrant of the MR vs. H plots. (For interpretation of the references to colour in this figure legend, the reader is referred to the web version of this article.)

MR_{INT} can be determined using the relations

$$MR_{SPT} = -\int_0^H f(k)dk \tag{3}$$

$$MR_{INT} = -JH - KH^3 \tag{4}$$

For the La-doped compound, the experimental MR vs. H curves fitted well with the Eq. (1) and from the fitting parameters MR_{SPT} has been determined which has come out to be 1.7% at 30 kOe. This very small value of MR_{SPT} indicates the presence of small ferromagnetic clusters. On the contrary, for the $x = 0$ sample this model does not fit well. This data fitted well with the mean field model ($MR \propto H^2$) which signifies that sample is purely in the paramagnetic phase at 300 K.

To explore the corresponding evolution in magnetic properties, we have measured the temperature dependent magnetization [M(T)] in zero field cooled warming (ZFC) and field cooled warming (FCW) protocols (see Fig. 4) in presence of 1 kOe external magnetic field. From the M(T) data two points are similar for both the compounds. First, a sharp increase of magnetization in both ZFC and FCW data at ~150 K and secondly, the bifurcation between the ZFC and FCW magnetization below 45 K (T_2). Such nature of the magnetization may be associated with some kind of glassy magnetic state of the compound[36,37]. The peak at 45 K is possibly due to the ordering of Pr^{3+} ions. Similar kind of the magnetic state for such compound was reported earlier also[9]. In addition to the above-mentioned characteristics, for $x = 0.2$ compound, a predominant magnetization value was observed in a large temperature span (from 150 K to 320 K). The broadening of the temperature is probably linked with the formation of the ferromagnetic clusters as evidenced by the magnetotransport study and the growth of these clusters take place at T^*. The different transition temperatures have been marked in the inset of Fig. 4(a). Our experimental results indicate that low temperature magnetization is reduced in La-doped compound. We have further studied the isothermal magnetization with magnetic field at 3 K [see Fig. 4(b)]. It shows that at the higher magnetic field region the magnetization value in the La-doped compound is a little bit smaller than that of $x = 0$ compound (inset of Fig. 4(b)). This reduction may be associated with the nonmagnetic character of La^{3+} in place of Pr^{3+} ions. Additionally, almost no hysteresis was found for both the samples.

From the Arrott plot [38] (inset I of Fig. 4(c)) it can be seen that high field slope of the M^2 vs. H/M curve do not intersect in the positive M^2 axes. It indicates the absence of any spontaneous magnetization in $x = 0.2$ compound at 300 K. Thus, the increase of magnetization at the high temperature region is due to the formation of the ferromagnetic clusters which grows in size with reduction of the temperature and creates long range ordering. To get further insight into the systems, and considering the clusters to be nearly noninteracting at the high temperature region ($T > 280$ K) we have analyzed the M(H) data of the compounds with Wohlfarth's model [39].where 'N' is the cluster density i.e. number of cluster per unit volume, '$\langle\mu\rangle$' is the average magnetic moment of the clusters and L(x) is the Langevin function. Both the M(H) data fitted well with the model (see Fig. 4)) and extracted '$\langle\mu\rangle$' and 'N' has been plotted in the inset (II) of Fig. 4(c). Here it can be clearly seen that the size of the clusters in $x = 0.2$ compound is higher than the parent compound.

$$M = N\langle\mu\rangle L\left(\frac{\langle\mu\rangle H}{k_B T}\right) \tag{5}$$

The presence of the short-range ferromagnetic clusters has also been confirmed from the temperature dependent thermoremanent magnetization (TRM) measurement. For this measurement, sample was cooled from well above the transition temperature ($T > 310$ K) in presence of different applied field and then after switching off the magnetic field at 2 K the magnetization was measured in the warming cycle and it has been presented in the Fig. 4(d). It being a zero field measurement, the paramagnetic susceptibility is likely to be suppressed in this case. The upturn of the susceptibility occurs for both the samples at ~50 K and ~150 K which was also observed in M(T) data (see Fig. 4(a)). On the other hand an another upturn is observed from 310 K in $x = 0.2$ compound which signifies the possible signature of the presence of ferromagnetic clusters.

Above all experimental outcomes infers that in $x = 0.2$ compound, even at high temperature predominant magnetization persist. Since magnetocaloric entropy change is directly related to the change of magnetization with respect to temperature, so it is expected that magnetocaloric effect will also be modified with respected to its parent compound $x = 0$. To estimate the magnetocaloric entropy change (ΔS_M) of the materials, field dependence of magnetization has been measured at different temperatures in ZFC protocol and before each successive measurement the sample was heated above the room temperature to destroy the signature of any magnetic history. The magnetocaloric entropy change was calculated from the Maxwell's thermodynamic relation

$$\Delta S_M = \int_0^H (\partial M/\partial T)dH \tag{6}$$

Temperature dependence of $-\Delta S_M$ for both the compounds with different external magnetic field is shown in Fig. 5(a) and (b). It is worth mentioning that the numerical value of $-\Delta S_M$ is reduced for the doped compound but the distribution of $-\Delta S_M$ in temperature scale is enhanced compared to $Pr_{0.8}Sr_{0.2}MnO_3$. Moreover, doping leads to a table-like MCE with a plateau in $-\Delta S_M$ vs. T curve over a wide temperature range (200 K to 320 K) for 5 kOe applied magnetic field. The width of

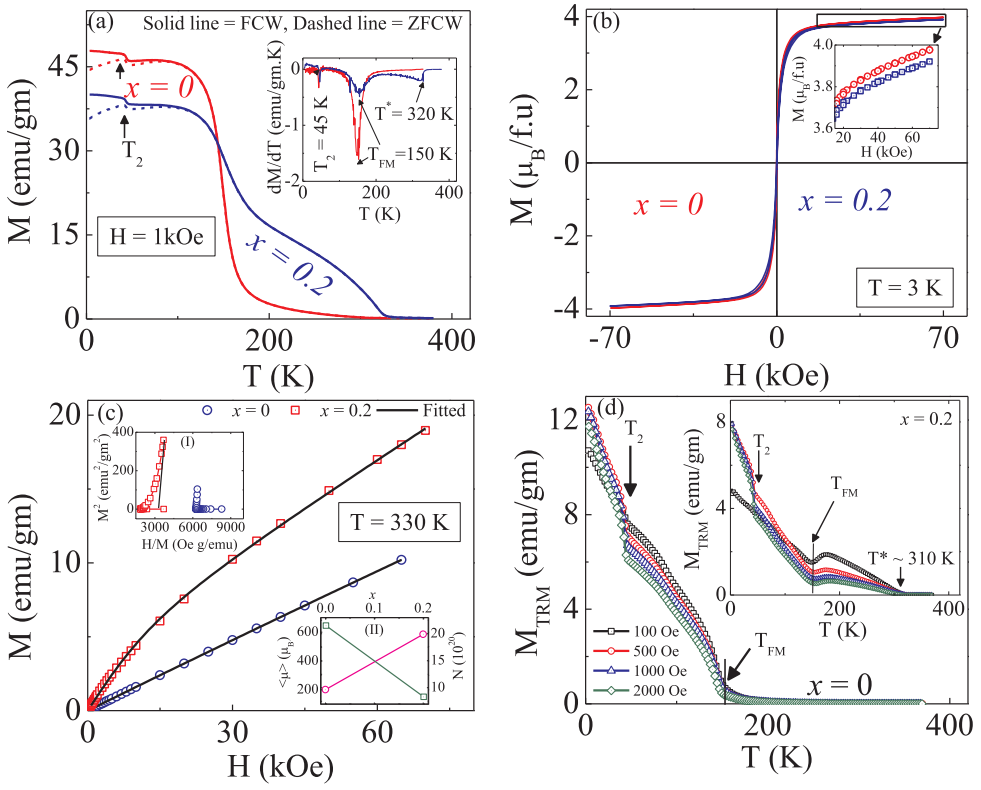

Fig. 4. (a) Temperature dependent magnetization in ZFCW and FCW protocols in presence of 1 kOe external magnetic field for the polycrystalline $Pr_{0.8-x}La_xSr_{0.2}MnO_3$ ($x = 0$, 0.2) compounds. Inset shows the transition temperatures in the dM/dT vs. T plots of the corresponding FCW curves. (b) Field dependence of the magnetization at 3 K for the $Pr_{0.8-x}La_xSr_{0.2}MnO_3$ ($x = 0$, 0.2) compounds. Inset is the enlarged view of M(H) at the higher field region. (c) Fittings of the M vs. H data, taken at 330 K for the polycrystalline $Pr_{0.8-x}La_xSr_{0.2}MnO_3$ ($x = 0$, 0.2) compounds, with Wohlfarths model where black lines are the corresponding fitted lines. Inset (I) presents the Arrott plots (M^2 vs H/M) of the samples. Inset (II) shows the evolution of the average cluster size and density for the compounds. (d) Temperature dependent of thermoremanent magnetization (M_{TRM}) measured in different cooling fields for the $x = 0$ compound. Inset shows the variation of M_{TRM} vs. T for the $x = 0.2$ compound measured in the same protocol as for $x = 0$.

this plateau is found to decrease with applied magnetic field but remains finite even for 70 kOe field. The table-like MCE avoids generation of the irreversible work and therefore is one of the major requirement in the Ericsson cycle, a basic cycle for magnetic refrigeration technology. Recently, table-like MCE have also been reported by R. M'nassri [40] and Wang et al. [41] by mixing two different composites. However, their different thermal and electrical conductivity is a drawback for utilization. In that sence our La-doped compound serve the purposes. Another important parameter in magnetic refrigeration is relative cooling power (RCP), which is defined as $RCP = -\Delta S_{M,max} \times \delta T_{FWHM}$ where δT_{FWHM} is the full width at half maxima of $-\Delta S_M$ vs T curves. The magnetic field dependence of RCP for both the compounds has been depicted in Fig. 5(b). An enhancement of RCP from 289 J/kg to 371 J/kg at 50 kOe field and from 423 J/kg to 635 J/kg at 70 kOe field is observed in the La-doped compound. Moreover, these values are large enough compared to other manganites reported in literature (for comparison see Table 2). Although, the $-\Delta S_{M,max}$ (for $x = 0.2$) is lower compared to some reported room temperature MCE materials but RCP is high in the La-doped compound and therefore this results shows a way of enhancing RCP of the materials.

Here another point needs to mention that in some cases RCP leads to an overestimation of material performance [47–49]. To quantify the material performance Wood and Potter [50] proposed a dimensionless figure, Coefficient of Refrigerant Performance (CRP), by normalizing with the positive work done on the refrigerant:

$$CRP = \frac{\Delta S_{max} \Delta T_{max}}{\int_0^{B_{max}} M(T_C, B) dB} \quad (7)$$

To see the efficiency of our samples, we have also calculated CRP for both the compounds and corresponding variation with external magnetic field is shown in the inset (II) of Fig. 5(c). It can be clearly seen that at higher magnetic field ($\geqslant$ 50 kOe) in the $x = 0.2$ compound there is also an enhancement of CRP like RCP.

To explore more insight about the state of magnetization using magnetocaloric effect as a tool, we have plotted $-\Delta S_M$ as a function of H^2 for both compounds at 300 K. According to the mean field theory [51], in paramagnetic state $-\Delta S_M \propto H^2$. Although, for the parent $x = 0$ compound, the linear behavior was observed, but there is the deviation from linearity in case of the $x = 0.2$ compound (shown in Fig. 5(c)). We have also fitted the isothermal magnetization data above the ordering temperature for the samples with the power law $-\Delta S_M \propto H^n$ and plotted the corresponding power 'n' with temperature in the inset of Fig. 5(c). For $x = 0$ compound, the power 'n' gradually reaches to the paramagnetic value '2'. Whereas for $x = 0.2$ compound the non monotonous behavior is observed and moreover it does not reach to the value '2' even at 330 K. Such nature again indicates the presence of short range magnetic correlation in $Pr_{0.6}La_{0.2}Sr_{0.2}MnO_3$ compound.

4. Conclusions

In summary, the present study on the structural, magnetic, magnetotransport and magnetocaloric properties of the polycrystaline $Pr_{0.8-x}La_xSr_{0.2}MnO_3$ ($x = 0$, 0.2) compounds, indicates that the chemical pressure change the ground state of ferromagnetic insulator ($x = 0$) to ferromagnetic metallic state ($x = 0.2$). The study also shows the appearance of the ferromagnetic clusters in the paramagnetic region of the $Pr_{0.6}La_{0.2}Sr_{0.2}MnO_3$ compound and is responsible for the enhancement of magnetoresistance and relative cooling power.

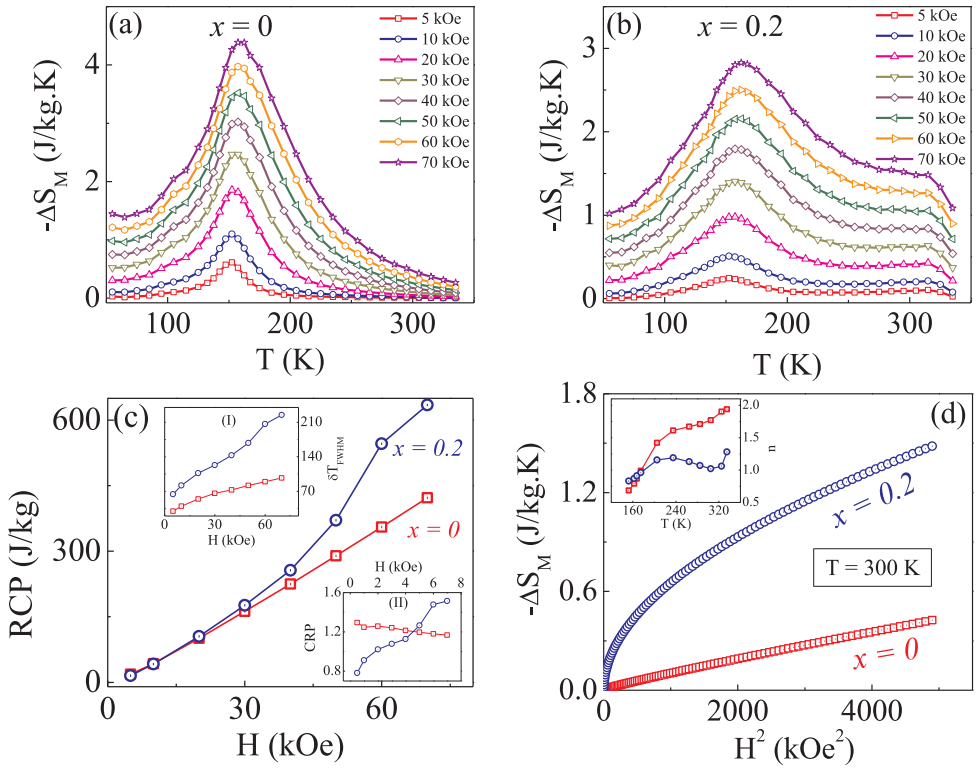

Fig. 5. Temperature dependent magnetocaloric entropy change for different external magnetic field for (a) $x = 0$ and (b) $x = 0.2$ compounds. (c) Variation of RCP with H at 300 K for the $Pr_{0.8-x}La_xSr_{0.2}MnO_3$ ($x = 0.0, 0.2$) compounds. Inset (I) and (II) shows the variation of δT_{FWHM} and CRP with H for $x = 0$ and 0.2 compounds (d) Plot of $-\Delta S_M$ vs. H^2 at 300 K for the $Pr_{0.8-x}La_xSr_{0.2}MnO_3$ ($x = 0.0, 0.2$) compounds. Inset shows the evolution of 'n' with the temperature ($T > T_{FM}$). All the insets in (c) and (d) with red and blue curves are for $x = 0$ and 0.2 compounds respectively. (For interpretation of the references to colour in this figure legend, the reader is referred to the web version of this article.)

Table 2
Comparison the values of $-\Delta S_{M,max}$ (J/kg-K) and *RCP* (J/kg) of $Pr_{0.6}La_{0.2}Sr_{0.2}MnO_3$ with some other manganites reported in literature.

Sample	T_C (K)	ΔH (kOe)	$-\Delta S_{M,max}$ (J/kg-K)	*RCP* (J/kg)	Reference
$La_{0.67}Ca_{0.33}MnO_3$	257	50	2.06	175	[42]
$La_{0.87}Sr_{0.13}MnO_3$	197	50	5.80	232	[43]
$La_{0.84}Sr_{0.16}MnO_3$	244	50	5.85	240	[43]
$La_{0.67}Sr_{0.33}MnO_3$	348	50	1.69	211	[42]
$La_{0.67}Ba_{0.33}MnO_3$	292	50	1.48	161	[42]
$Pr_{0.7}Sr_{0.14}Ba_{0.16}MnO_3$	202	50	4.80	258	[23]
$Pr_{0.775}Sr_{0.225}MnO_3$	175	50	3.59	292	[45]
$La_{0.67}Sr_{0.33}Mn_{0.9}Cr_{0.01}O_3$	328	50	5.0	200	[44]
$La_{0.7}Sr_{0.3}Mn_{0.98}Ni_{0.02}O_3$	350	50	6.52	>222, < 337	[46]
$La_{0.6}Pr_{0.1}Sr_{0.3}MnO_3$	345	15	2.52	48.41	[34]
$Pr_{0.8}Sr_{0.2}MnO_3$	150	15	1.50	72	This work
$Pr_{0.6}La_{0.2}Sr_{0.2}MnO_3$	150	15	0.75	71	This work
$Pr_{0.8}Sr_{0.2}MnO_3$	150	50	3.54	289	This work
$Pr_{0.6}La_{0.2}Sr_{0.2}MnO_3$	150	50	2.17	371	This work

Acknowledgement

The work was supported by Department of Atomic Energy (DAE), Govt. of India.

References

[1] C.N.R. Rao, R. Raveau (Eds.), Colossal Magnetoresistance, Charge ordering and Related Properties of Manganese Oxides, World Scientific, Singapore, 1998.
[2] S.W. Cheong, H.Y. Hwang, Y. Tokura (Ed.), Contribution to Colossal Magnetoresistance Oxides, Monographs in Condensed Matter Science, Gordon and Breach, London, 1999.
[3] Y. Tokura, Colossal Magnetoresistive Oxides, Gordon and Breach Science, Amsterdam, 2000.
[4] Y. Tokura, Reports Prog. Phys. 69 (2006) 797.
[5] J.F. Mitchell, D.N. Argyriou, C.D. Potter, D.G. Hinks, J.D. Jorgensen, S.D. Bader, Phys. Rev. B 54 (1996) 6172.
[6] M. Paraskevopoulos, F. Mayr, J. Hemberger, A. Loidl, R. Heichele, D. Maurer, V. Müller, A.A. Mukhin, A.M. Balbashov, J. Phys. Condens. Matter 12 (2000) 3993.
[7] W. Prellier, M. Rajeswari, T. Venkatesan, R.L. Greene, Appl. Phys. Lett. 75 (1999) 1446.
[8] M. Pissas, G. Papavassiliou, J. Phys. Condens. Matter 16 (2004) 6527.
[9] C. Martin, A. Maignan, M. Hervieu, B. Raveau, Phys. Rev. B 60 (1999) 12191.
[10] Y. Tomioka, A. Asamitsu, H. Kuwahara, Y. Moritomo, Y. Tokura, Phys. Rev. B 53 (1996) R1689.
[11] S. Banik, I. Das, RSC Adv. 7 (2017) 16575.
[12] S. Banik, N. Banu, I. Das, J. Alloys Compd. 745 (2018) 753.
[13] A.M. Tishin, Y.I. Spinchkin, The Magnetocaloric Effect and its Applications, IOP, Bristol, 2003.
[14] K.A. GschneidnerJr, V.K. Pecharsky, A.O. Tsokol, Reports Prog. Phys. 68 (2005) 1479.
[15] N.A. de Oliveira, P.J. von Ranke, Phys. Rep. 489 (2010) 89.
[16] N.S. Bingham, M.H. Phan, H. Srikanth, M.A. Torija, C. Leighton, J. Appl. Phys. 106

(2009) 023909.
[17] X.Q. Zheng, J. Chen, J. Shen, H. Zhang, Z.Y. Xu, W.W. Gao, J.F. Wu, F.X. Hu, J.R. Sun, B.G. Shen, J. Appl. Phys. 111 (2012) 07A917.
[18] S. Pakhira, C. Mazumdar, R. Ranganathan, S. Giri, M. Avdeev, Phys. Rev. B 94 (2016) 104414.
[19] O. Tegus, E. Brück, K.H.J. Buschow, F.R. de Boer, Nature 415 (2002) 150.
[20] M.H. Phan, M.B. Morales, N.S. Bingham, H. Srikanth, C.L. Zhang, S.W. Cheong, Phys. Rev. B 81 (2010) 94413.
[21] L. Zhang, C. Israel, A. Biswas, R.L. Greene, A. de Lozanne, Science 80 (298) (2002) 805.
[22] A. Biswas, S. Chandra, T. Samanta, B. Ghosh, S. Datta, M.H. Phan, A.K. Raychaudhuri, I. Das, H. Srikanth, Phys. Rev. B 87 (2013) 134420.
[23] S. Banik, I. Das, J. Alloys Compd. 742 (2018) 248.
[24] S. Banik, K. Das, T. Paramanik, N.P. Lalla, B. Satpati, K. Pradhan, I. Das, NPG Asia Mater. 10 (2018) 923930.
[25] T. Krenke, E. Duman, M. Acet, E.F. Wassermann, X. Moya, L. Mañosa, A. Planes, Nat. Mater. 4 (2005) 450.
[26] A. Rostamnejadi, M. Venkatesan, J. Alaria, M. Boese, P. Kameli, H. Salamati, J.M.D. Coey, J. Appl. Phys. 110 (2011) 43905.
[27] M. Quintero, J. Sacanell, L. Ghivelder, A.M. Gomes, A.G. Leyva, F. Parisi, Appl. Phys. Lett. 97 (2010) 121916.
[28] C.N.R. Rao, A.K. Cheetham, R. Mahesh, Chem. Mater. 8 (1996) 2421.
[29] J. Chen, X.Q. Zheng, Q.Y. Dong, J.R. Sun, B.G. Shen, Appl. Phys. Lett. 99 (2011) 122503.
[30] M. Moumen, A. Mehri, W. Cheikhrouhou-Koubaa, M. Koubaa, A. Cheikhrouhou, J. Alloy. Compd. 509 (2011) 9084.
[31] P.K. Siwach, H.K. Singh, O.N. Srivastava, J. Phys. Condens. Matter 20 (2008) 273201.
[32] C.A.F. Vaz, F.J. Walker, C.H. Ahn, S. Ismail-Beigi, J. Phys. Condens. Matter 27 (2015) 123001.
[33] A. Urushibara, Y. Moritomo, T. Arima, A. Asamitsu, G. Kido, Y. Tokura, Phys. Rev. B 51 (1995) 14103.
[34] Y. Zhang, P.J. Lampen, T.L. Phan, S.C. Yu, H. Srikanth, M.H. Phan, J. Appl. Phys. 111 (2012) 063918.
[35] P. Raychaudhuri, K. Sheshadri, P. Taneja, S. Bandyopadhyay, P. Ayyub, A.K. Nigam, R. Pinto, S. Chaudhary, S.B. Roy, Phys. Rev. B 59 (1999) 013919.
[36] K. Mydeen, P. Mandal, D. Prabhakaran, C.Q. Jin, Phys. Rev. B 80 (2009) 14421.
[37] D.N.H. Nam, R. Mathieu, P. Nordblad, N.V. Khiem, N.X. Phuc, Phys. Rev. B 62 (2000) 8989.
[38] A. Arrott, Phys. Rev. 108 (1957) 1394.
[39] E.P. Wohlfarth, J. Appl. Phys. 29 (1958) 595.
[40] R. Mhassri, J. Supercond. Nov. Mag. 29 (2016) 207–213.
[41] G.F. Wang, Z.R. Zhao, H.L. Li, X.F. Zhang, Ceram. Int. 41 (2015) 9035–9040.
[42] D.T. Morelli, A.M. Mance, J.V. Mantese, A.L. Micheli, J. Appl. Phys. 79 (1996) 373.
[43] A. Szewczyk, H. Szymczak, K. Piotrowski, Appl. Phys. Lett. 77 (2000) 1026.
[44] Y. Sun, W. Tong, Y.H. Zhang, J. Magn. Magn. Mater. 232 (2001) 205.
[45] S. Banik, I. Das, J. Magn. Magn. Mater. 460 (2018) 234.
[46] M.H. Phan, N.D. Tho, N. Chau, S.C. Yub, M. Kurisu, J. Appl. Phys. 97 (2005) 103901.
[47] A. Smith, C.R.H. Bahl, R. Bjørk, K. Engelbrecht, K.K. Nielsen, N. Pryds, Adv. Energy Mater. 2 (2012) 1288–1318.
[48] F. Guillou, H. Yibole, G. Porcari, L. Zhang, N.H. van Dijk, E. Brück, J. Appl. Phys. 116 (2014) 063903.
[49] L.D. Griffith, Y. Mudryk, J. Slaughter, V.K. Pecharsky, J. Appl. Phys. 123 (2018) 034902.
[50] M.E. Wood, W.H. Potter, Cryogenics 25 (1985) 667.
[51] H. Oesterreicher, F.T. Parker, J. Appl. Phys. 55 (1984) 4334.